Earth Planets Space, **61**, 83–91, 2009

Magnetic properties and archeointensity determination on Pre-Columbian pottery from Chiapas, Mesoamerica

Juan Morales[1,2], Avto Goguitchaichvili[1,2*], Guillermo Acosta[3], Tomas González-Moran[1], Luis Alva-Valdivia[1], Jasinto Robles-Camacho[4], and Ma. del Sol Hernández-Bernal[5]

[1]*Instituto de Geofísica, Universidad Nacional Autónoma de México, Ciudad Universitaria s/n, 04510, MEXICO DF, México*
[2]*Laboratorio Interinstitucional de Magnetismo Natural, Instituto de Geofísica, Sede Michoacán, Universidad Nacional Autónoma de México, Morelia, Michoacán, México*
[3]*Instituto de Investigaciones Antropológicas, Universidad Nacional Autónoma de México, Ciudad Universitaria s/n, 04510, MEXICO DF, México*
[4]*Laboratorio de Arqueometría del Occidente, INAH-Morelia, Michoacán, México*
[5]*Instituto de Geología, Universidad Nacional Autonoma de México, Ciudad Universitaria s/n, 04510, MEXICO DF, México*

(Received December 6, 2007; Revised February 27, 2008; Accepted March 3, 2008; Online published January 23, 2009)

As part of the effort to establish an archeointensity variation curve for Mesoamerica, 13 archeologically well-identified pottery samples belonging to the Ocozocoautla site (Chiapas) were studied. Analyzed samples consist of 'ofrenda type' pottery fragments found in several caves. Three archeological intervals are involved: 450–100 B.C., 200–550 A.D. and 550–900 A.D. The Thellier method in its modified form was applied to small fragments previously embedded in salt pellets. Raw intensity values were further corrected for cooling rate effects. The common time-consuming TRM anisotropy correction protocol was substituted by an alternative approach during the paleointensity experiments. Forty-two specimens, belonging to six samples, yielded high-quality Thellier determinations. The NRM fraction f used for paleointensity determination ranges between 0.42 to 0.99, and the quality factor q (Coe *et al.*, 1978) varies from 4 to 59, being normally greater than 5. These results correspond to data of good quality. The mean archeointensity values per pottery fragments range from 14.6±1.5 to 59.5±13.8 μT, while the corresponding virtual axial dipole moments range from 2.5±0.3 to 10.0±2.4 $\times$ 10^{22} A m^2. These new data, although not numerous, are of high quality and definitively contribute to the Mesoamerican, still insipient, archeointensity database.

Key words: Archeointensity, Mesoamerica, Pre-Columbian pottery, thermoremament magnetization, Chiapas.

1. Introduction

Systematic geomagnetic field measurements in Mexico began at the end of the 17th century at Teoloyucan geomagnetic observatory—a member of the *Intermagnet* worldwide network (http://132.248.6.186/). The evolution of the geomagnetic field prior to times of direct instrumental measurement is studied by analyzing remanent magnetization of archeological material, lava flows and lake sediments.

Archeomagnetic research was initiated in France in the 1930s with the pioneering work of E. Thellier (see Chauvin *et al.*, 2000). Nowadays, a relatively high number of archeomagnetic determinations have been accumulated. However, their geographic distribution is still highly uneven since most investigations are concentrated in Europe (Korte *et al.*, 2005, see also Fig. 1).

Mexico, as whole Mesoamerica, may still be considered as *terra incognita* from the archeomagnetic point of view. With the exception of studies of recent volcanoes (Nagata *et al.*, 1965; Bucha *et al.*, 1970; Lee, 1975; Aitken *et al.*, 1991; Gonzalez *et al.*, 1997; Böhnel *et al.*, 1997; Morales *et al.*, 2001; Böhnel *et al.*, 2003; Morales *et al.*, 2006), no serious attempts have been undertaken to study the rich cultural heritage of the region. The study reported here presents the first archeointensity survey from Mesoamerica and is part of the effort to establish an archeointensity variation curve for the region. We present here results of six (out of 13 analyzed) archeologically well controlled fragments from the Ocozocoautla archeological site (Chiapas, southern Mexico). Samples consist of 'ofrenda-type' potteries fragments found in several caves. Three archeological intervals are involved: 450–100 B.C., 200–550 A.D. and 550–900 A.D.

The mean archeointensity values per pottery fragments range from 14.6±1.7 to 59.5±13.8 μT, while the corresponding virtual axial dipole moments (VADMs) range from 2.5±0.3 to 10.0±2.4 $\times$ 10^{22} A m^2. The low value here presented correlates in time with those reported by Bucha *et al.* (1970), for which a low average intensity for Mexico at about 600 A.D. was suggested. These data, although limited in number, are new and of high quality, and they contribute to the local archeointensity database.

Attempts to date the studied ceramics by means of global field curves (McElhinny and Senanayake, 1982; Yang *et al.*, 2000) revealed that these curves were of little use for

*Also at sabatic at Departamento de Geologia y Mineralogia, Instituto de Investigaciones Metalurgicas, Universidad Michoacana San Nicolas de Hidalgo.

Table 1. List of studied sites and corresponding samples.

Archaeological site	UTM coordinates	Sample	Ceramic type	Prehispanic period
Cueva Petapa	E0445986 N1842124	PCTA002	Yomonó inciso	Early Classic
		PCTA003	Paniagua inciso	Early Classic
Cueva Escondida	E0459702 N1840290	PCTA005	Pobacama arenoso	Protoclassic
El Retazo	E455645 N1872029	PCTA008	Tonapac burdo	Early Classic
Sima del Tigre	E0445807 N1858512	PCTA011	Kocakpan alisado	Late Classic–Early Post Classic
El panal	E0440215 N1844875	PCTA010	Vicente café	Late Preclassic

Table 2. Relative chronology of ceramic samples in regional context.

Archaeological period	Ceramic phase	Range	Radiocarbon dates[1]
Early Post Classic		900–1300 A.D.	
Late Classic	Jama	550–900 A.D.	720±90 A.D.[2]
Early Classic	Cauta and Nuti	200–550 A.D.	385±90 A.D.[2]
			450±110 A.D.[3]
Protoclassic	Horcones and Istmo	200 A.D.–100 B.C.	115±95 A.D.[2]
Late Preclassic	Pompac	100 B.C.–450 B.C.	320±100 B.C.[2]
			330±130 B.C.[2]

[1]Not Calibrated. [2]Lee (1974). [3]Agrinier (1975).

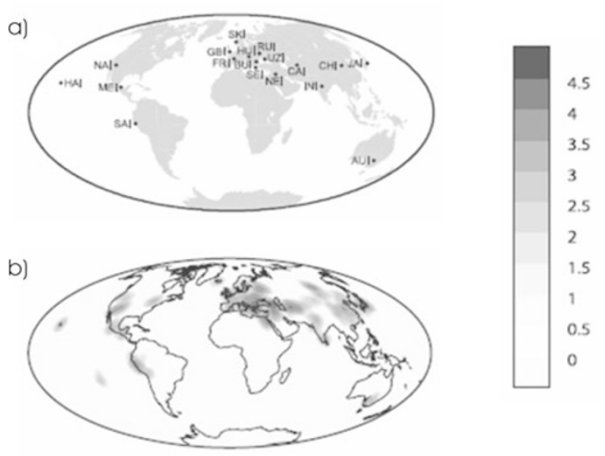

Fig. 1. (a) Locations of regions yielding archeoinetensity results. (b) Worldwide archeointensity data distribution and corresponding concentration, modified from Korte *et al.* (2005).

this propose, emphasizing the great need for a regional archeointensity reference curve.

2. Study Area and Archeological Context

The study area is located within the Grijalva-Usumacinta hydrological system, in the close vicinity of a small town (Ocozocoautla), 25 km to the west of Tuxtla Gutierrez (capital of Chiapas State) (Fig. 2).

Although Chiapas ceramics have been studied since the 19th century, these investigations are still very scarce (Culbert, 1965). Among the early works, those reported by Schumann (1936) and Weiant (1943) deserve a special mention. Later, Shook (1956) and Adams (1959) described few sites in central Chiapas (namely along the Pan-American Highway) belonging to the Pre-Classic (1600 B.C.–100 B.C.) and Protoclassic periods (100 B.C.–200 A.D.). Culbert (1965) provided a first analytical description of ceramics found in the Chiapas highland making evident a regional differentiation between the Classic (200–900 A.D.) and Post-Classic periods (900–1521 A.D.). Special efforts were paid to the Chiapa de Corzo archeological complexes (Fig. 2), which constitute at least 200 structures disposed around '*patios*' or squares. The age interval from 1600 to 1450 B.C. is considered to provide the first evidence of the ceramic production in the region (Clark and Cheetham, 2005). This period is characterized by small agricultural villages and an early stage of ceramic production—a common feature of both Chiapas and Guatemala. Large spherical narrow-mouth '*tecomates*' and some primitive vessels are the most common vestiges. Between approximately 1150 and 450 B.C., Chiapa de Corzo and Mirador became the largest ceremonial centers in the *Depresión Central* region (Agrinier, 1975). The increase in inhabitants is manifested by the presence of numerous platforms and terraces with public architecture. The privileged geographical situation in terms of proximity to the Grijalva and La Venta rivers allowed the inhabitants to control the sailing and the road traffic. In the Late Pre-classic (450 B.C.–100 B.C.) period, the cultural exchange was enlarged with the current states of Tabasco, Veracruz and Oaxaca and probably also with Campeche, Yucatan and the Péten area (Dixon, 1959). Generally speaking, this region seems to represent a local ceramic tradition, but one also related to a series of similar traditions in southern Mexico.

The samples analyzed in our study come from five archaeological sites located in the region of Ocozocoautla

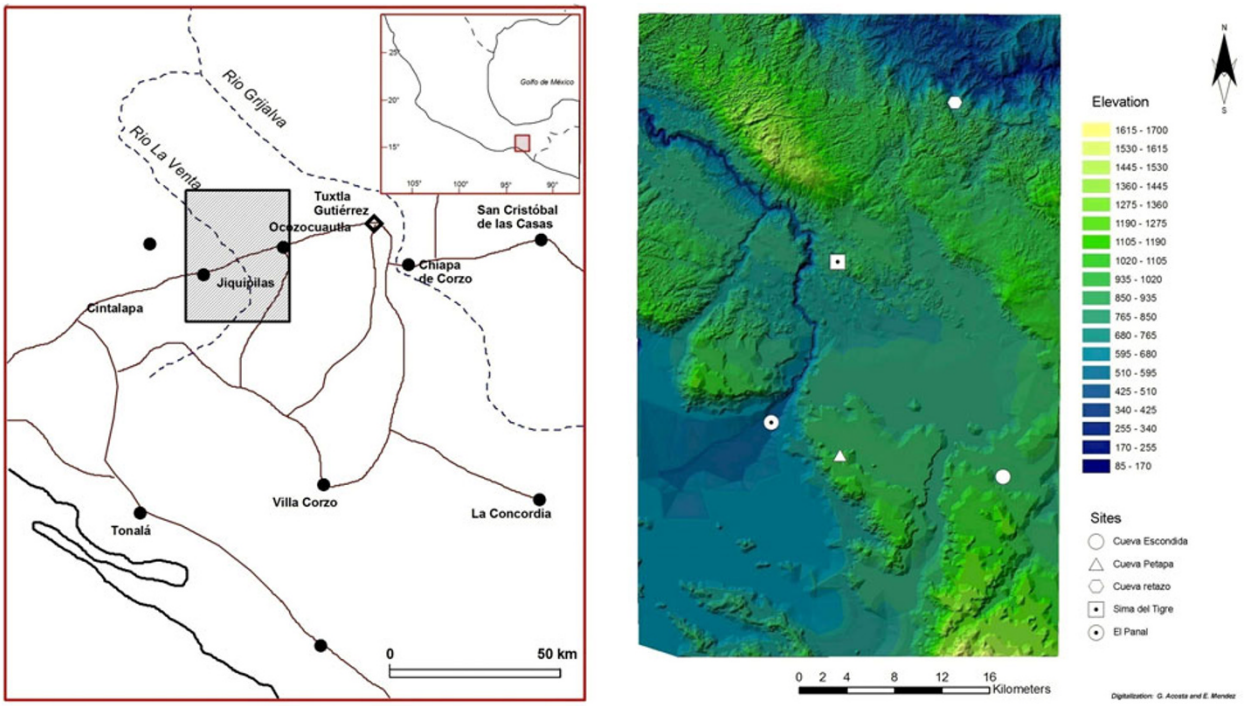

Fig. 2. Map of Ocozocoautla region. Left: Shaded rectangle represents the study area. Right: Study area detail and archaeological sites.

Fig. 3. Ceramic offering of an undisturbed context in El Retazo Cave.

(Table 1, see also Fig. 2). Three of these sites (Cueva Escondida, Petapa and El Retazo) are humid caves in which ceramic offerings have been found in their interior (Fig. 3). Sima del Tigre is a cenote-like formation, typical of the karstic regions of southern Mexico, but without the presence of an underground river in its interior; there, domestic ceramic remains are associated with rock art and no other archaeological feature. El Panal is an open site that includes archaeological remains associated to a small domestic mound.

All of the ceramic samples were recovered during the surface survey season in autumn 2005, and their age was estimated by typological comparison with other ceramics in the area. It is necessary to point out that reliable ceramic chronological markers exist in the region (Clark and Cheetham, 2005; Bryant *et al.*, 2005), and they allow us to assign each sample to its corresponding period with relative confidence. Radiocarbon dates associated to similar ceramic types have also been obtained in the region (Table 2).

3. Experimental Procedure

3.1 Remanence properties

In order to retrieve the magnetic history experienced by the samples after their elaboration and to check their magnetic stability, a thermal treatment (up to 600°C, using an ASC Thermal Demagnetizer) was applied to pilot samples of each potsherd groups. Measurements of remanent magnetization were carried out using a JR6 spinner magnetometer. These experiments revealed the presence of more than one magnetic component in some samples, suggesting possible post-heatings of the artifacts or the acquisition of viscous remanent magnetizations (Fig. 4(a)). Six out of 13 samples show an essentially single magnetic component pointing through the origin (Fig. 4(b)). The median destructive field ranges from 20 to 40 mT, suggesting a small pseudo-single domain structure of magnetic carries (Dunlop and Özdemir, 1997).

3.2 Susceptibility vs. temperature experiments

Continuous low-field susceptibility vs. temperature curves in air were carried out on all 13 pottery fragments in order to estimate the magnetic mineralogy and thermal stability. For this purpose, a home-made automated 'High Moore' susceptibility bridge was employed using a controlled heating-cooling rate of 20°C/min. The measurements were performed on a separated magnetic fraction of the samples due to the extremely low signal of bulk samples. Generally speaking, the studied samples yield simple magnetic mineralogy. Ti-poor titanomagnetites seem to be the principal magnetic carriers (Fig. 5). Heating and cool-

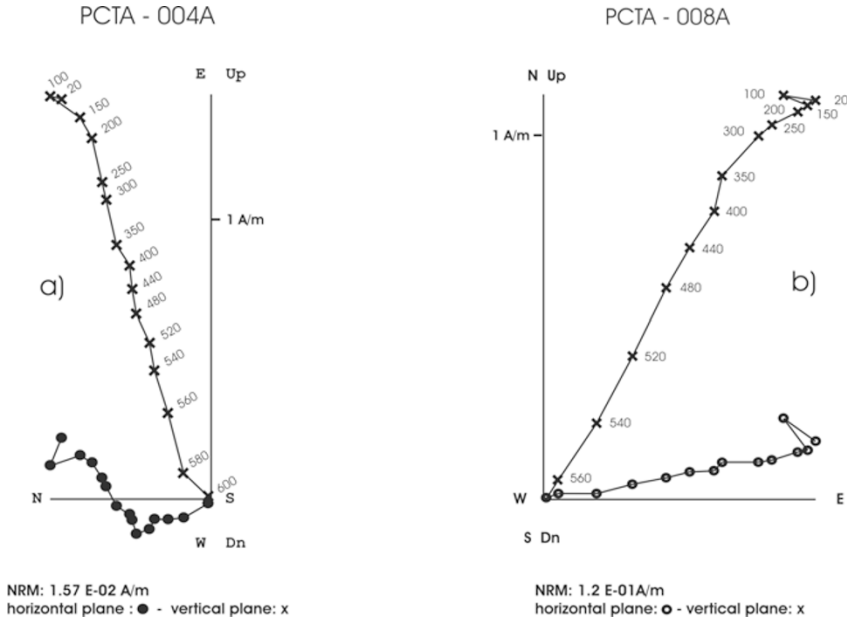

Fig. 4. Representative orthogonal vector demagnetization plots. (a) Example of multicomponent magnetization. (b) Example of essentially one-component magnetization. Numbers indicate the corresponding temperature step in degrees Celsius.

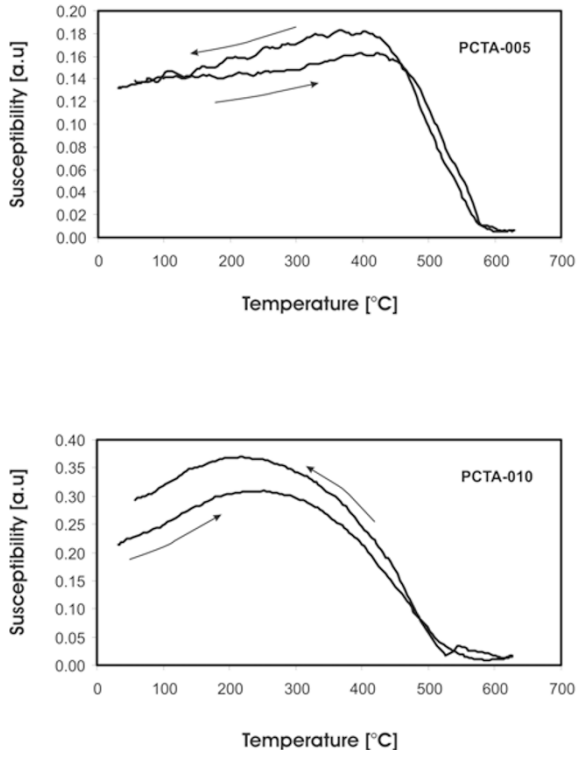

Fig. 5. Representative continuous susceptibility versus temperature curves. Arrows indicate the heating and cooling paths.

ing paths are reasonably reversible, which indicate to relatively high thermomagnetic stability and, therefore, that the samples are potentially suitable for archeointensity determinations using Thellier double heating method.

3.3 Hysteresis curves

Attempts to estimate the domain state and/or mineralogical composition of archeological samples by means of hysteresis parameters seems to be even more difficult than in rocks or synthetic samples (e.g., Aitken *et al.*, 1991; Chauvin *et al.*, 2000; Genevey and Gallet, 2002). This difficulty is basically due to the nature of the primary material (mud/clay) used for the elaboration of archeological artifacts. Consequently, a selection criterion of 'potentially suitable' samples for archeointensity studies was based principally on AF/thermal demagnetization treatment and continuous thermomagnetic curves. Nonetheless, hysteresis and IRM measurements were done on all 13 samples using an AGFM 'Micromag' apparatus with fields up to 1.2 Tesla. Saturation remanent magnetization (J_{rs}), saturation magnetization (J_s) and coercitive force (H_c) were calculated after correction for the paramagnetic contribution. Coercivity of remanence (H_{cr}) was determined by applying a progressively increasing backfield after saturation. Representative hysteresis and IRM curves at are shown in Fig. 6. Hysteresis curves are symmetrical in all cases, and there are no clear potbellied or wasp-waisted behaviors (Tauxe *et al.*, 1996), probably indicates restricted ranges of opaque mineral coercivities. Corresponding isothermal remanence (IRM) acquisition curves seem to be very similar for all samples. Saturation is reached in moderate fields of the order of 150–200 mT, which points to some spinels as remanence carriers.

4. Archeointensity Determination

Six out of thirteen potteries showing no evidence of strong secondary overprints according to thermal demagnetization and yielding reasonably reversible thermomagnetic curves were selected for archeointensity (AI) experiments. Each fragment was further divided in at least seven specimens and then 'packed' into ultra pure salt (NaCl) pellets in order to treat them as standard paleomagnetic cores. In total, we obtained 42 specimens. Magnetization per unit volume of 'blank' pellets ranges on the order of 10^{-5} A/m, whereas magnetization of typical archaeomagnetic cores

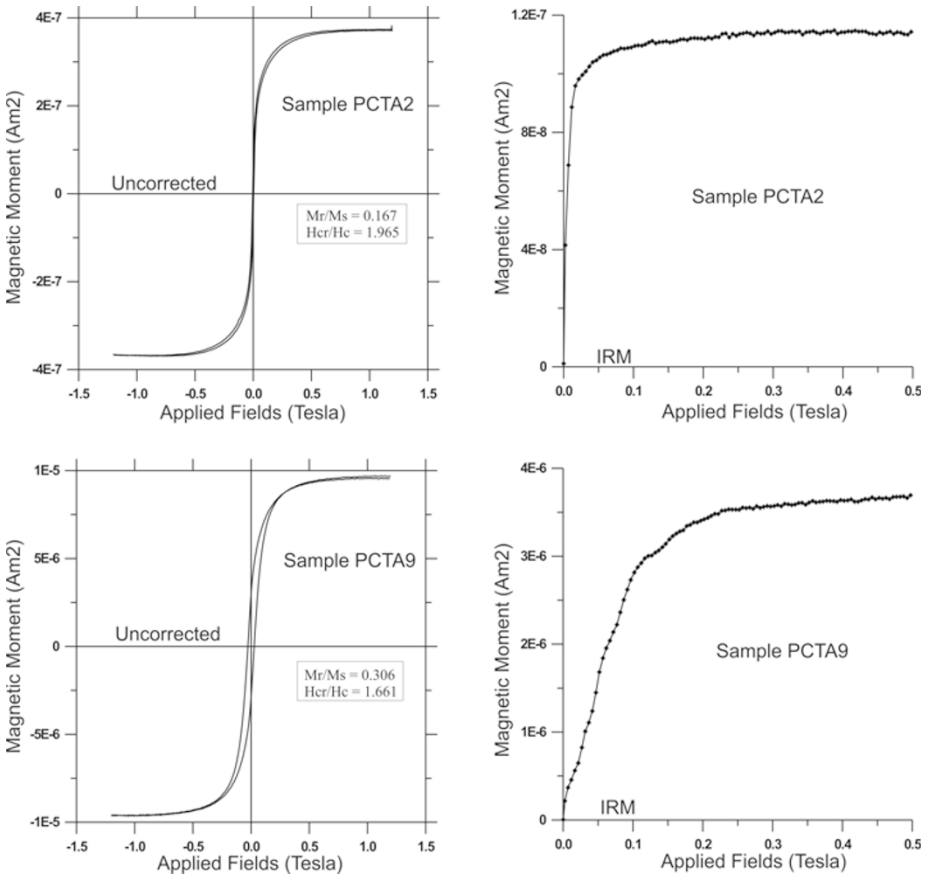

Fig. 6. Representative hysteresis and corresponding isothermal remanent acquisition plots.

prepared for AI determinations ranges on the order of 10^{-2} to 10^{-1} A/m. The AI experiments were performed following the Thellier method (Thellier and Thellier, 1959) in its modified form (Coe, 1967). Twelve increasing temperature steps were distributed through the whole temperature spectrum during the AI experiments. The pTRM checks were performed at every two steps.

5. Cooling Rate and Anisotropy Correction

Cooling rate dependence of TRM was investigated following a modified procedure described in Chauvin *et al.* (2000). TRM gained during last step of the Thellier experiment (575°C) was subsequently designated as TRM_1. At the same temperature, a new full TRM (TRM_2) was given to all samples but this time using a long cooling time (∼10 h). Finally, a third TRM (TRM_3) was created using the same cooling time (of about 45 min) as that used to create TRM_1. The effect of cooling rate upon TRM intensity was estimated by calculating the percentage variation between the intensity acquired during a short and a long cooling time (TRM_1 and TRM_2). Changes in TRM acquisition capacity were estimated by means of the percentage variation between the intensity acquired during same cooling time (TRM_1 and TRM_3). Cooling rate correction was applied only when the corresponding change in TRM acquisition capacity was below 15%.

TRM anisotropy corrections can be implemented in different ways (e.g. McCabe *et al.*, 1985; Selkin *et al.*, 2000; Chauvin *et al.*, 2000, among others). It essentially requires the creation of a TRM along six mutually perpendicular directions ($+X$, $+Y$, $+Z$, $-X$, $-Y$, $-Z$) by cooling them from 600°C to room temperature in a known magnetic field. This involves six additional heatings, which may significantly alter the magnetic mineralogy of the samples. To circumvent this time-consuming procedure, individual specimens (belonging to the same fragment) were embedded into the salt pellet in the six above-described positions. In this way, possible bias due to TRM anisotropy effects would be canceled, as attested by the results of our various previous test experiments. Numerous ceramic fragments broken into six pieces were thermally demagnetized for this purpose. Sister samples were later embedded into salt pellets and aligned along one of the above-described positions taking as a reference the flattening plane of the ceramic fragment. Specimens elaborated in such a way were remagnetized by applying a constant magnetic field along the Z-axis of the pellet and were later measured. In general, specimens oriented parallel to the easy plane of magnetization (flattening plane) yielded relatively higher intensities than those oriented perpendicular to it, with differences lower than 10%. We then carried out a pseudo Thellier-Coe experiment with these specimens. Averaged 'ancient' intensities reproduced the laboratory field used to remagnetize the specimens within 2%.

6. Main Results and Discussion

Archeointensity results are summarized in Table 3, and representative Arai plots are shown in Fig. 7. These data

Table 3. Summary of archeointensity experiments: T_{min}–T_{max}, temperature range used for AI estimation; n, number of NRM-TRM points used for the determination; UC: uncorrected; CRC: cooling rate corrected; $H_{ant\ UC}$, uncorrected archeointensity; $\sigma H_{ant\ UC}$, standard deviation of $H_{ant\ UC}$; $H_{ant\ CRC}$, cooling rate corrected archeointensity; H_{accept}, accepted AI after CRC and acceptance criteria application; f, g and q: fraction of extrapolated NRM used for intensity determination, gap and quality factor (Coe *et al.*, 1978), respectively; VADM: virtual axial dipole moment. The laboratory field was set to 30 μT during the experiment.

	H_{lab} [μT]	= 30	N	= 12						
Sample	T_{min}–T_{max}	n	$H_{ant\ UC}$ [μT]	$\sigma H_{ant\ UC}$ [μT]	$H_{ant\ CRC}$ [μT]	H_{accept} [μT]	f	g	q	VADM [A m^2]
pcta02-1	300–475	6	73.05	5.82	46.8	46.8	0.647	0.774	6.28	8.2E+22
pcta02-2	300–475	6	88.95	3.21	68.3	68.3	0.511	0.768	10.87	1.2E+23
pcta02-3	300–475	5	63.51	3.51	44.8	44.8	0.582	0.705	7.42	7.8E+22
pcta02-4	300–475	6	64.05	5.01	50.3	50.3	0.452	0.763	4.41	8.8E+22
pcta02-5	*300–475*	*6*	*72.75*	*8.49*	*58.2*		*0.442*	*0.764*	*2.89*	
pcta02-6	300–575	10	87.96	7.56	69.4	69.4	0.797	0.796	7.38	1.2E+23
pcta02-7	300–575	10	96.54	6.9	77.2	77.2	0.702	0.745	7.32	1.3E+23
		Mean =	78.1		59.3	59.5	0.6	0.8	6.7	1.0E+23
		σ =	13.0		12.6	13.8	0.1	0.0	2.5	
pcta03-1	400–565	8	18.03	0.63	15.6	15.6	0.524	0.832	12.48	2.7E+22
pcta03-2	400–565	8	19.14	1.26	16.6	16.6	0.567	0.843	7.26	2.9E+22
pcta03-3	350–565	9	17.58	1.14	15.4	15.4	0.571	0.859	7.56	2.7E+22
pcta03-4	400–565	8	14.28	0.78	12.4	12.4	0.517	0.841	7.96	2.2E+22
pcta03-5	400–565	8	14.49	1.05	12.7	12.7	0.511	0.844	5.95	2.2E+22
pcta03-6	350–565	9	16.80	1.11	14.7	14.7	0.549	0.852	7.08	2.6E+22
pcta03-7	*350–565*	*8*	*16.17*	*1.59*	*14.7*		*0.491*	*0.836*	*4.17*	
		Mean =	16.6		14.6	14.6	0.5	0.8	7.5	2.5E+22
		σ =	1.8		1.5	1.7	0.0	0.0	2.5	
pcta08-2	300–565	10	48.06	1.59	41.0	41.0	0.653	0.882	17.4	17.2E+22
pcta08-3	300–565	10	62.25	3.63	54.1	54.1	0.688	0.885	10.44	9.4E+22
pcta08-5	300–565	10	61.92	2.55	54.7	54.7	0.639	0.877	13.61	9.5E+22
pcta08-6	300–565	10	55.89	2.49	49.9	49.9	0.622	0.882	12.31	8.7E+22
pcta08-7	300–565	10	56.76	3.24	52.3	52.3	0.546	0.863	8.25	9.1E+22
pcta08-8	300–565	10	54.75	2.10	46.3	46.3	0.744	0.874	16.95	8.1E+22
		Mean =	56.6		49.7	49.7	0.6	0.9	13.2	8.7E+22
		σ =	5.2		5.2	5.2	0.1	0.0	3.6	
pcta09-1	300–565	10	27.99	1.98	25.2	25.2	0.986	0.841	11.72	4.4E+22
pcta09-2	300–565	10	30.45	2.07	27.5	27.5	0.962	0.846	11.97	4.8E+22
pcta09-3	20–565	11	27.93	1.92	24.9	24.9	0.968	0.868	12.22	4.3E+22
pcta09-4	20–565	11	28.68	1.92	25.9	25.9	0.926	0.872	12.06	4.5E+22
pcta09-5	20–565	11	28.38	2.13	25.4	25.4	0.978	0.87	11.34	4.4E+22
pcta09-6	20–565	11	28.05	2.07	25.3	25.3	0.983	0.87	11.59	4.4E+22
pcta09-8	20–565	11	27.81	2.13	25.1	25.1	0.994	0.866	11.24	4.4E+22
		Mean=	28.5		25.6	25.6	1.0	0.9	11.7	4.5E+22
		σ =	0.9		0.9	0.9	0.0	0.0	0.4	
pcta10-1	300–525	8	80.61	3.18	65.6	65.6	0.387	0.836	8.20	1.1E+23
pcta10-2	300–525	8	67.68	4.80	53.8	53.8	0.441	0.816	5.07	9.4E+22
pcta10-3	300–525	8	63.93	4.32	51.8	51.8	0.47	0.814	5.66	9.0E+22
pcta10-4	300–475	7	67.59	4.11	56.8	56.8	0.398	0.795	5.20	9.9E+22
pcta10-5	300–550	9	60.60	3.33	50.5	50.5	0.473	0.834	7.18	8.8E+22
pcta10-6	300–475	8	54.57	2.91	45.4	45.4	0.491	0.818	7.53	7.9E+22
pcta10-7	300–565	10	52.32	1.47	44.7	44.7	0.522	0.829	15.40	7.8E+22
		Mean=	63.9		52.6	52.6	0.5	0.8	7.8	9.2E+22
		σ =	9.5		7.2	7.2	0.0	0.0	3.6	
pcta11-1	300–575	10	54.87	0.96	49.3	49.3	0.674	0.845	32.55	8.6E+22
pcta11-3	300–575	11	52.98	0.87	49.6	49.6	0.689	0.883	37.05	8.6E+22
pcta11-4	300–565	10	52.65	0.66	50.0	50.0	0.853	0.869	59.13	8.7E+22
pcta11-5	300–565	10	48.69	1.44	43.9	43.9	0.646	0.859	18.76	7.6E+22
pcta11-6	300–565	10	44.97	1.11	39.5	39.5	0.652	0.864	22.82	6.9E+22
pcta11-7	300–565	9	62.82	2.31	56.7	56.7	0.807	0.857	18.81	9.9E+22
pcta11-8	300–575	11	49.41	0.78	45.3	45.3	0.791	0.871	43.6	47.9E+22
		Mean=	52.8		48.2	47.8	0.7	0.9	33.3	8.3E+22
		σ =	6.0		5.9	5.5	0.1	0.0	14.8	

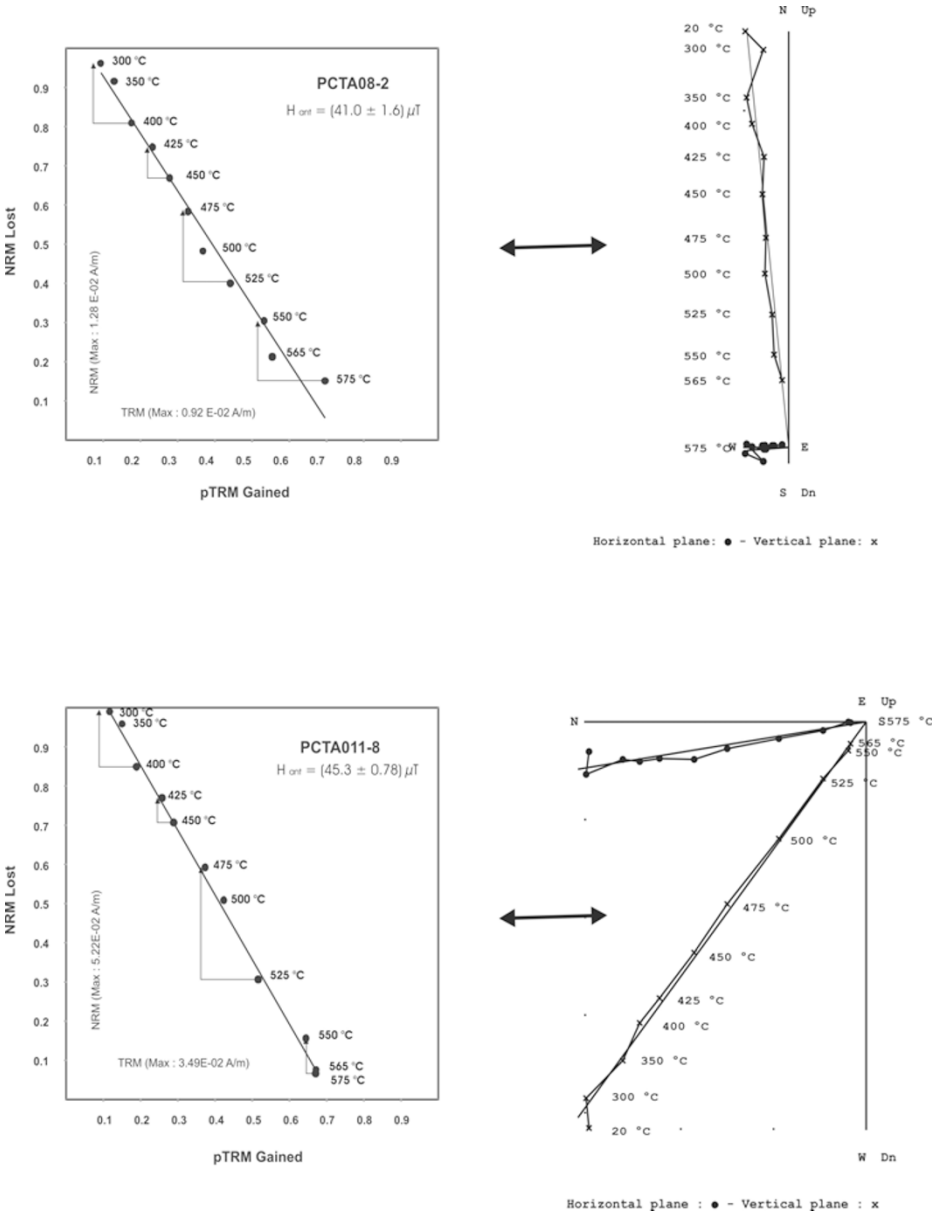

Fig. 7. Typical NRM-TRM diagrams (so-called Arai-Nagata plots) and associated Zijderveld diagrams of NRM end points. (Same notation as in Fig. 4 applies for Zijderveld diagrams).

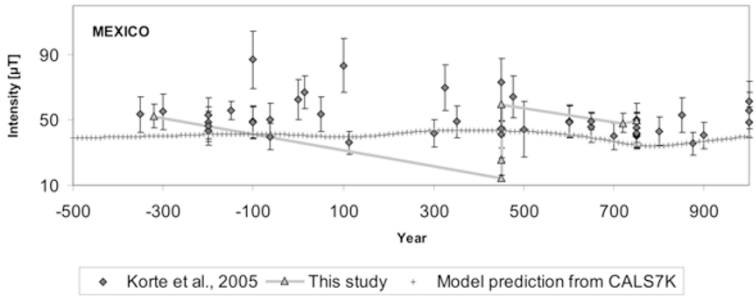

Fig. 8. Archeointensity data for Mexico modified from Korte *et al.* (2005). Crossed line represents model prediction from CALS7K.2 (Korte and Constable, 2005).

were gathered according to strict—nowadays commonly used—individual determinations acceptance criteria: (1) At least five NRM-TRM points (9 on average) are used for archeointensity determination; (2) Fraction (f) of the NRM used for calculation (see in Coe *et al.*, 1978) is greater than 0.3 (0.6 on average); (3) Coe's quality factor 'q' ranges from 6 up to 30; (4) positive pTRM checks.

Cooling rate corrected values are 16% lower than corre-

sponding raw intensities in most cases, and scatter in mean value is systematically reduced by the application of the CR correction. However, an increase of up to 24% (on average) in TRM intensity was detected for one case (sample PCTA02).

TRM anisotropy effects are assumed to be small since scatter in the mean value (small standard deviation of the mean) is within 10%, in accordance with previous test experiments. The only exception is sample PCTA02. In general, the studied samples yield low within-fragment dispersion, thereby supporting the above assumption, and mean archeointensity values are rather accurately determined.

However, two samples belonging to 'Cueva Petapa' (PCTA002 and PCTA003), both assigned to the same chronological context, yielded significantly different intensity values (59.5 and 14.6 μT, respectively). We interpret these results as evidence of a mixing of potteries with very distinct ages. No alternative evidence could be found to explain this difference between archeointensity values since the remanence as well as rock magnetic properties of both samples seem to be quite similar.

Mean archeointensity values per pottery fragments range from 14.6±1.7 to 59.5±13.8 μT while corresponding VADMs range from 2.5±0.3 to 10.0±2.4 $\times$ 10^{22} A m^2. These new data, although not numerous, are of high quality and definitively contribute to the Mesoamerican, still insipient, archeointensity database. Mean archeointensities obtained here (except for one ceramic fragment) closely follow the trend of existing archeointensity results for the region (Fig. 8). It should be noted that most data complied by Korte and Constable (2005) for the first millennium correspond to determinations made in the early 1960s and 1970s (Nagata *et al*., 1965; Bucha *et al*., 1970; Lee, 1975). Thus, no cooling rate or anisotropy corrections were applied.

Comparison of old and new data against the prediction of model CALS7K for the past 7 millennia reveals a markedly offset downwards, especially for the past 5 millennia. As we already mentioned above, there is no alternative credible reason to try to explain the very different AI values for samples belonging to the Cueva Petapa. Data of Bucha *et al*. (1970) suggest, however, a low average intensity for Mexico at about 600 A.D., and also a relatively fast transition from approximately 200 A.D. to 600 A.D., with intensity varying from almost twice the present value to somewhat lower than the present one, which is in agreement with Nagata's data (Nagata *et al*., 1965). These facts may support the possibility of a mixing of pottery fragments.

An attempt to date the studied ceramics by means of reported global field curves (McElhinny and Senanayake, 1982; Yang *et al*., 2000) failed, probably due to their low resolution. Relatively better approximation may be obtained by using local field curves for North and South America (Bowles *et al*., 2002) where a fast transition for the first millennium is also observed.

We conclude that Mesoamerican potteries from Chiapas show a great usefulness for archeointensity studies. The archeointensity determinations obtained here represent the first high-quality data for the region since cooling rate and anisotropy corrections are applied. While geomagnetic field models are an excellent way to model the behavior of the Earth's magnetic field on a large scale, they do not have the enough accuracy for dating an archeological structure (Zanarini *et al*., 2007), which emphasizes the strong need for a regional archeointensity reference curve.

Acknowledgments. We wish to thank to Elena Zanella and Ana Ma. Sinito for their careful review of the manuscript. We also acknowledge Bertha Aguilar-Reyes for her valuable contribution to an early version of the manuscript and A. Gonzalez-Rangel for assistance with the experimental measurements. AG is grateful for financial support provided by CONACYT project #54957 and Proyecto Interno de Investigación 'G122'.

References

Adams, R. M., Report on an archeological reconnaissance in the Central Highlands of Chiapas, Mexico, Project of the Department of Anthropology of the University of Chicago, Chicago, 1959.

Agrinier, P., Mound 9 and 10 at Mirador, Chiapas, Mexico, *Papers of the New World Archeological Foundation*, Provo, Utah, **39**, 1975.

Aitken, M. J., L. J. Pesonen, and M. Leino, The Thellier paleointensity technique: Minisamples versus standard size, *J. Geomag. Geoelectr.*, **43**, 325–331, 1991.

Böhnel, H., J. Morales, C. Caballero, L. Alva, G. McIntosh, S. González, and G. Sherwood, Variation of Rock Magnetic Parameters and Paleointensities over a Single Holocene Lava Flow, *J. Geomag. Geoelectr.*, **49**, 523–542, 1997.

Böhnel, H., A. J. Biggin, D. Walton, J. Shaw, and J. A. Share, Microwave paleointensities from a recent Mexican lava flow, baked sediments and reheated pottery, *Earth Planet. Sci. Lett.*, **214**, 221–236, 2003.

Bowles, J., J. Gee, J. Hildebrand, and L. Tauxe, Archeomagnetic intensity results from Californiaand Ecuador: evaluation of regional data, *Earth Planet. Sci. Lett.*, **203**, 967–981, 2002.

Bryant, D. D., J. E. Clark, and D. Cheetham, Ceramic Sequence of the Upper Grijalva Region, Chiapas, México, *New World Archeological Foundation,* Provo, Utah, No. 67, 2005.

Bucha, V., R. E. Tylor, R. Berger, and E. W. Haury, Geomagnetic intensity: Changes during the past 3000 years in the western hemisphere, *Science*, **168**, 111–114, 1970.

Chauvin, A., A. Garcia, Ph. Lanos, and F. Laubenheimer, Paleointensity of the geomagnetic field recovered on archaeomagnetic sites from France, *Phys. Earth Planet. Inter.*, **120**, 111–136, 2000.

Clark, J. and D. Cheetham, La cerámica del Formativo en Chiapas, in: B. Carrion y A. García, La Producción Alfarera en el México Antiguo Vol. I, Colección Científica INAH, México, 285–243, 2005.

Coe, R. S., Paleo-Intensities of the Earth's Magnétic Field Determined from Tertiary and Quaternary Rocks, *J. Geophys. Res.*, **72**(12), 3247–3262, 1967.

Coe, R., S. Grommé and E. A. Mankinen, Geomagnetic paleointensity from radiocarbon-dated flows on Hawaii and the question of the Pacific nondipole low, *J. Geophys. Res.*, **83**, 1740–1756, 1978.

Culbert, P. T., The ceramic history of the Highlands of Chiapas, *Papers of the New World Archeological Foundation*, Provo, Utah, No. 19, 1965.

Dixon, K. A., Ceramic from two preclassic periods at Chiapa de Corzo, Chiapas, Mexico, *Papers of the New World Archeological Foundation*, Orinda, Ca, No. 5, 1959.

Dunlop, D. and Ö. Özdemir, *Rock-Magnetism, fundamentals and frontiers*, Cambrige University Press, 573pp, 1997.

Genevey, A. and Y. Gallet, Intensity of the geomagnetic field in western Europe over the past 2000 years: New data from ancient French pottery, *J. Geophys. Res.*, **107**(B11), 2285, doi:10.1029/2001JB000701, 2002.

Gonzalez, S., G. Sherwood, H. Böhnel, and E. Schnepp, Paleosecular variation in Central Mexico over the last 30 000 years: the record from lavas, *Geophys. J. Int.*, **130**, 201–219, 1997.

Korte, M. and C. G. Constable, Continuous geomagnetic field models for the past 7 millenia: 2. CALS7K, *Geochem. Geophys. Geosyst.*, **6**, Q02H16, doi:10.1029/2004GC000801, 2005.

Korte, M., A. Genevey, C. G. Constable, U. Frank, and E. Schnepp, Continuous geomagnetic field models for the past 7 millenia: 1. A new global data compilation, *Geochem. Geophys. Geosyst.*, **6**, Q02H15, doi:10.1029/2004GC000800, 2005.

Lee, S. S., Secular variation of the intensity of the geomagnetic field during the past 3,000 years in North, Central and South America, Ph.D. thesis, University of Oklahoma, Norman, 1975.

Lee, T., Mound 4 Excavations at San Isidro, Chiapas, Mexico, *Papers of*

the New World Archeological Foundation, Provo, Utah, No. 34, 1974.

McCabe, C., M. Jackson, and B. Ellwood, Magnetic anisotropy in the Trenton limestone: results of a new technique, anisotropy of anhysteric susceptibility, *Geophys. Res. Lett.*, **12**, 333–336, 1985.

McElhinny, M. W. and W. E. Senanayake, Variations in the geomagnetic dipole 1: the past 50,000 years, *J. Geomag. Geoelectr.*, **34**, 39–51, 1982.

Morales, J., A. Goguitchaichvili, and J. Urrutia-Fucugauchi, A rock-magnetic and paleointensity study of some Mexican volcanic lava flows during the Latest Pleistocene to the Holocene, *Earth Planets Space*, **53**(9), 893–902, 2001.

Morales, J., L. M. Alva-Valdivia, A. Goguitchaichvili, and J. Urrutia-Fucugauchi, Cooling rate corrected paleointensities from the Xitle lava flow: Evaluation of within-site scatter for single spot-reading cooling units, *Earth Planets Space*, **58**(10), 1341–1347, 2006.

Nagata, T., K. Kobayashi, and E. J. Schwarz, Archeomagnetic intensity studies of South and Central America, *J. Geomag. Geoelectr.*, **17**, 399–405, 1965.

Schumann, E. A., A recent visit to southern, *Mexico. Maya Res.*, **3**(3–4), 296–305, 1936.

Selkin, P. A., J. S. Gee, L. Tauxe, W. P. Meurer, and A. J. Newell, The effect of remanence anisotropy on paleointensity estimates: a case study from the Archean Stillwater Complex, *Earth Planet. Sci. Lett.*, **183**, 403–416, 2000.

Shook, E. M., An archeological reconnaissance in Chiapas, Mexico, *Papers of the New World Archeological Foundation*, Orinda, Ca, No. 1, 1956.

Tauxe, L., T. A. T. Mullender, and T. Pick, Pot-bellies, wasp-waists and superparamagnetism in magnetic hysteresis, *J. Geophys. Res.*, **95**, 12337–12350, 1996.

Thellier, E. and O. Thellier, Sur l'intensité du champ magnétique terrestre dans le passé historique et géologique, *Ann. Géophys.*, **15**, 285–376, 1959.

Weiant, C. W, An introduction to the ceramic of Tres Zapotes, Bulletin 139, Bureau of American Ethnology, Washington, 1943.

Yang, S., H. Odah, and J. Shaw, Variations in the geomagnetic dipole moment over the last 12 000 years, *Geophys. J. Int.*, **140**, 158–162, 2000.

Zananiri, I., C. M. Batt, Ph. Lanos, D. H. Tarling, and P. Linford., Archaeomagnetic secular variation in the UK during the last 4000 years and its application to archaeomagnetic dating, *Phys. Earth Planet. Inter.*, **160**, 97–107, 2007.

J. Morales (e-mail: jmorales@geofisica.unam.mx), A. Goguitchaichvili, G. Acosta, T. González-Moran, L. Alva-Valdivia, J. Robles-Camacho, and Ma. del Sol Hernández-Bernal